TELKOMNIKA, Vol.14, No.2, June 2016, pp. 613~621
ISSN: 1693-6930, accredited **A** by DIKTI, Decree No: 58/DIKTI/Kep/2013
DOI: 10.12928/TELKOMNIKA.v14i1.2749

Fusion of Infrared and Visible Images Based on Non-subsample Contourlet Transform

Tingman Zhang[1*], Qing Wang[2]
[1]Xi'an Innovation College, Yan'an University, Xi'an 710100, Shaanxi China
[2]School of Automation and Information Engineering, Xi'an University of Technology, Xi'an 710048, Shaanxi China
*Corresponding author, e-mail: 1464527907@qq.com

Abstract

For the single spectrum image could not fully express the target feature information, this paper proposed a multispectral image fusion method based on non-subsample contourlet transform (NSCT). For the low frequency coefficients decomposed, fourth-order correlation coefficient is used to calculate the correlation between each low frequency coefficients, averaging fusion for the higher correlation coefficient, weight phase congruency fusion for the low correlation coefficient. For high frequency coefficients, Gaussian weight sum modified Laplace method is used for fusing, to retain more local structure details. Simulation results show that the method effectively retain the image structure information and more local details, and increase the image contrast.

Keywords*: Image Fusion, NSCT, Weight Phase Congruency, Sum Modified Laplacian*

1. Introduction

Scene imaging of different spectral ranges has different characteristics. Infrared spectrum is quite sensitive to the temperature information and can image in the night vision while the visible image is strong in detail description, but weak in night-vision imaging quality; the fusion of infrared and visible images can overcome the shortcoming of single spectrum image and improve the image quality.

Contourlet transform is an image analysis tool under the framework of multi-scale geometric analysis. Compared with wavelet transform, Contourlet transform has better directivity and anisotropy [1]. Since it is not translation-invariant, Contourlet transform has pseudo-Gibbs phenomena in the singular point or line. Arthur and other people [2] have removed the sub-sampling process in the Contourlet transform creatively, proposed Nonsubsampled Contourlet Transform (NSCT), replaced the translation invariance at the cost of certain redundancy and eliminated the pseudo-Gibbs phenomena and it is applicable to the analysis of natural scene image. The image fusion method based on NSCT focuses on the combination of the decomposed low- and high-frequency coefficients according to certain rules. Literature [3-6] consider the pixel position information and think that the pixels which are closer to the central pixel has more significant impact on the central pixel and they use different fusion methods to low- and high-frequency coefficients and obtain better fusion effects. Literature [7] provides a new idea for the image fusion rules by using image quality evaluation to conduct iterative fusion to the images; however, structure similarity [8] (SSIM) has single computational scale; it doesn't consider the pixel position information and it has bad infrared image processing effect [9].

This paper integrates the 4th-order correlation coefficients and phase congruency and proposes a fusion method of infrared and visible images based on NSCT. It fuses the low-frequency coefficients with low correlation by using an improved phase congruency and the mean value of the coefficients with high correlation and perform fusion to the high-frequency coefficients with Gaussian weighting SML. The experiment shows that the fusion method of this paper can have better quantization result in different evaluation standards.

Received December 17, 2015; Revised March 19, 2016; Accepted April 6, 2016

2. Nonsub Sampled Contourlet Transform (NSCT)

NSCT is made up of NonsubSampled Pyramid (NSP) and NonsubSampled Directional Filter Bank (NSDFB), as indicated in Figure 1. The nonsubsampling process is realized by àtrous algorithm, which has low computational complexity. NSP mainly performs multi-resolution representation to the image and NSDFB realizes the translation invariance and obtains the presentation of high-frequency details.

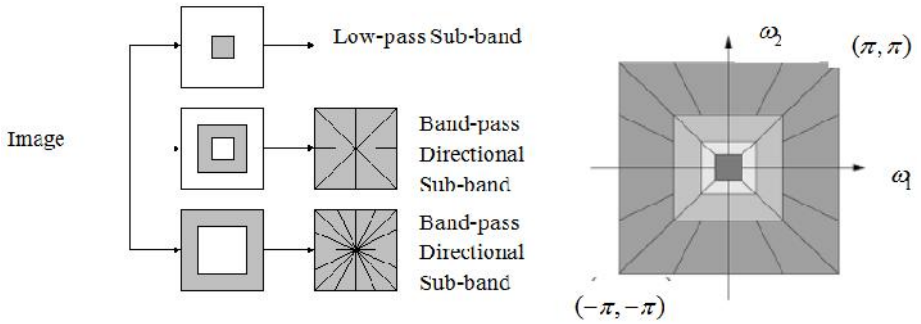

Figure 1. Constitution of NSCT

Figure 2 is the result of 2nd-order NSCT decomposition of Lena image. From the decomposition result, it can be seen that the high-frequency sub-band after the image pyramid is decomposed by NSDFB shows different directivity; therefore, NSCT can effectively detect such singular characteristics as the image curve.

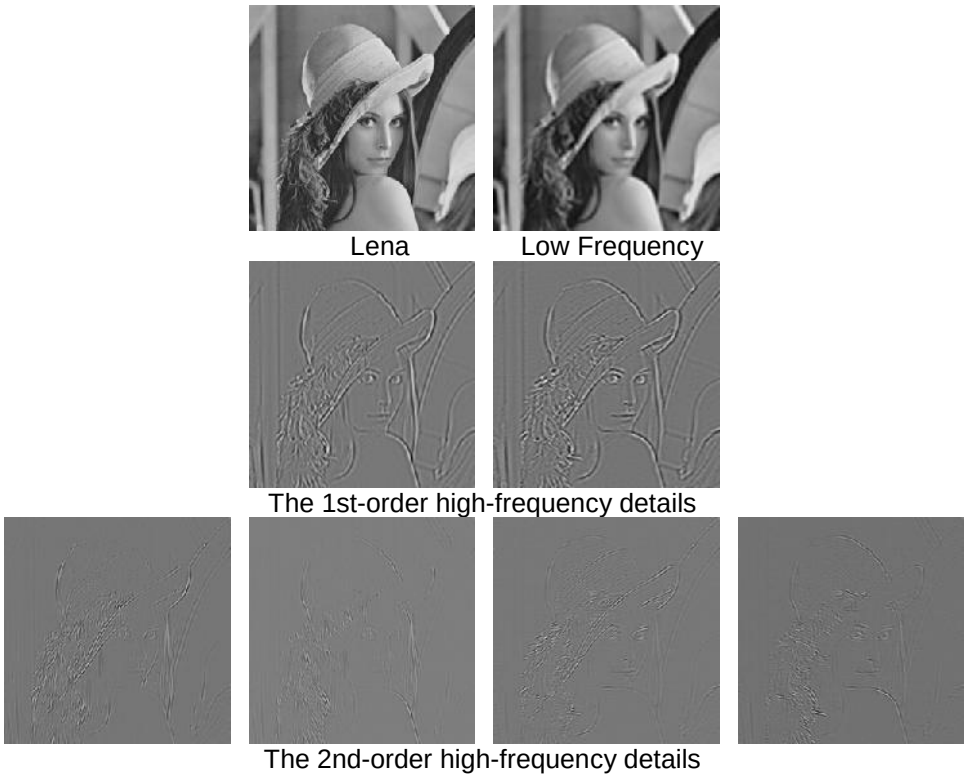

Figure 2. Result of 2nd-order nsct decomposition of lena

3. Design of Fusion Rule

3.1, Low-Frequency Coefficient Fusion Based on Weight Phase Congruency

The low-frequency coefficients after NSCT decomposition include the main image energy and it can be seen as the approximate component of the image. For the different spectral imaging of the same scene, the decomposed low-frequency coefficients have different correlation. The component with low correlation means bigger differences in the image while the component with high correlation means that the image has approximate structure. This paper fuses the component with low correlation and the component with high correlation by using weight phase congruency and taking mean value respectively [10].

The physiological and psychological research results demonstrate that the characteristics that people pay attention to have certain phase congruency in the image frequency domain, namely that the points with phase congruency include the important image feature information [11]. The theory of phase congruency (PC) builds the model of mammals recognizing object features. It is a means to measure the significance of the local image structure and it has nothing to do with dimension. Different from the common models which define the image feature where the image grayscale changes, PC model defines the image feature in the maximum phase value. It is defined as Formula (1): $E(x)$ is the root mean square of the sum of the filter responses in different scales, $A_n(x)$ is the room mean square of the filter response in certain scale, n is the scale and £ is a non-zero constant.

$$PC(x) = \frac{E(x)}{£ + \sum_n A_n(x)} \tag{1}$$

The calculation of the image filter responses in different scales chooses the common-used log-Gabor filter in the image analysis field. Its two-dimensional frequency domain representation is indicated as Formula (2):

$$G_2(\mu, ¯) = \exp\left(-\frac{\left(\log(\mu/\mu_0)\right)^2}{2±_r^2}\right) \cdot \exp\left(-\frac{\left(¯ - ¯_j\right)^2}{2±_-^2}\right) \tag{2}$$

Here, μ_0 is the center frequency of the filter, $±_r$ controls the bandwidth of the filter, $¯_j$ is the Azimuth of the filter, $¯_j = j® / J \quad j = \{0,1,\ldots,J-1\}$, J is the number of the Azimuths and $±_-$ control the angle bandwidth of the Azimuth of the filter. Figure 3 is the three-dimensional diagram of log-Gabor filter frequency domain.

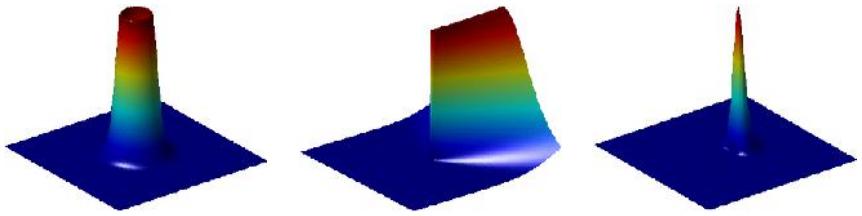

(a) Radial component (b) Phase component (c) log-gabor filter

Figure 3. Three-dimensional diagram of log-gabor filter

For the 2D image $f(x)$, M_n^o and M_n^e are the orthogonal odd- and even- symmetry filters constructed by log-Gabor filter in the scale n respectively. To change the filter frequency-domain responses by adjusting μ_0 and $¯_j$ convolves M_n^o and M_n^e with image $f(x)$ and obtains the filter response in Point x, which his shown as Formula (3):

$$\left[e_{n,¯_j}(x), o_{n,¯_j}(x)\right] = \left[f(x) * M_n^e, f(x) * M_n^o\right] \tag{3}$$

The amplitude response and energy under different directions and scales are indicated as follows:

$$A_{n,-_j}(x) = \sqrt{e_{n,-_j}(x)^2 + e_{o,-_j}(x)^2} \tag{4}$$

$$E_{-_j}(x) = \sqrt{\left(\sum_n e_{n,-_j}(x)\right)^2 + \left(\sum_n e_{o,-_j}(x)\right)^2} \tag{5}$$

According to Formula (1), the PC value of 2D image signal is as follows:

$$PC_{2D}(x) = \frac{\sum_j E_{-_j}(x)}{£ + \sum_j \sum_n A_{n,-_j}(x)} \tag{6}$$

Given the position information of the image pixel, this paper weights by using the phase congruency Gaussian function performs on low-frequency coefficients and proposes Gauss Weight Phase Congruency (GWPC) to measure the image structure features. The Gaussian function used in this paper is as follows:

$$G(x) = e^{\left(-\frac{X}{2\pm^2}\right)} \tag{7}$$

Therefore, the representation formula of the low-frequency coefficient GWPC is indicated as follows:

$$S_{GWPC}(x) = PC_{low}(x)G_{low}(x) \tag{8}$$

It can be seen from the above PC theory model that PC value reflects the sensitivity of different image structures on human vision and it is the important basis to measure the image structure features. As for different image structure region, the calculation result of GWPC is demonstrated as Figure 4.

As for the correlation measure of low-frequency coefficients, this paper uses the 4th-order correlation coefficient [12] which has excellent detail description ability to measure the correlation of infrared and visible images and it is defined as follows:

$$C_{A,B}(x) = \frac{\sum_{y\in\Omega}\left(A(y) - «_A\right)^2\left(B(y) - «_B\right)^2}{\sqrt{\left[\sum_{y\in\Omega}\left(A(y) - «_A\right)^4\right]\left[\sum_{y\in\Omega}\left(B(y) - «_B\right)^4\right]}} \tag{9}$$

Here, $«_A$ and $«_B$ are the image mean. The relationship between the low-frequency coefficient C_{low}^F by integrating correlation and GWPC and the low-frequency coefficients C_{low}^A and C_{low}^B of the source image is as follows:

$$C_{low}^F = \begin{cases} \dfrac{C_{low}^A + C_{low}^B}{2} & C_{A,B} > T_h \\ w_A C_{low}^A + w_B C_{low}^B & C_{A,B} \le T_h \end{cases} \tag{10}$$

As for the coefficient with high correlation between infrared and visible images, it is fused by taking the mean; otherwise, it is fused by weight GWPC. The weight uses the form indicated as the formula below:

$$w_A = \frac{S_{GWPC}^A}{S_{GWPC}^A + S_{GWPC}^B}, \quad w_B = 1 - w_A \tag{11}$$

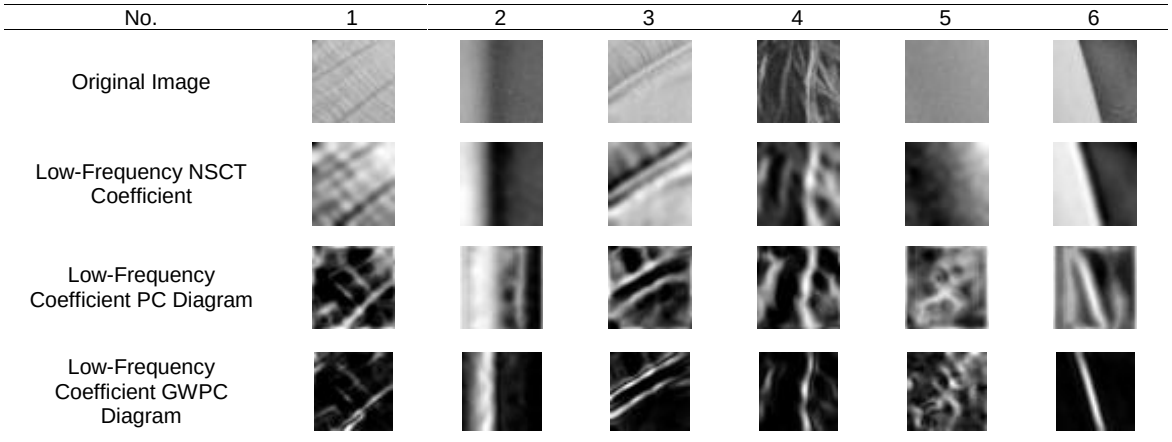

Figure 4. Image phase congruency diagram of different structure features

3.2. High-Frequency Coefficient Fusion Based on Gauss Weight SML

The high-frequency coefficients decomposed by NSCT represent the detail information of infrared and visible images. The fusion method to choose the maximum absolute value doesn't take the impact of the neighborhood pixels into consideration and as an operation method based on points, this method is easy to be affected by noises. Sum Modified Laplacian (SML) better reflects the edge features of different image structures and it can represent the image sharpness and definition. This paper fuses high-frequency coefficients via Gauss weight SML, which is defined as follows:

$$SML^{l,k}(i,j)=\sum_{a=-P}^{P}\sum_{b=-Q}^{Q}\left[ML^{l,k}(i+a,j+b)\right]^2 \tag{12}$$

$$ML^{l,k}(i,j)=\left|2H^{l,k}(i,j)-H^{l,k}(i-r,j)-H^{l,k}(i+r,j)\right|+\left|2H^{l,k}(i,j)-H^{l,k}(i,j-r)-H^{l,k}(i,j+r)\right| \tag{13}$$

Here, $H^{l,k}$ is the 1st-order k-direction high-frequency sub-band coefficient after NSCT decomposition and r is the radius of the neighborhood window. Formula (12) doesn't take the influence of the pixel position into account. Literature [13] proposes a normalized SML (NSML), introduces position information into ML through weighting matrix and emphasizes the contribution of the pixels at different distances to the central pixel. This literature uses the following weight formula:

$$\left[\mu(a,b)\right]_{(2P+1)\times(2Q+1)}=\frac{1}{\sum_{a=-P}^{P}\sum_{b=-Q}^{Q}\hat{W}(a,b)}\hat{W}_{(2P+1)\times(2Q+1)} \tag{14}$$

$$\hat{W}_{(2P+1)\times(2Q+1)}=X^{T}Y \tag{15}$$

Here, $X=[1,2,\ldots,P+1,\ldots,2,1]_{1\times(2P+1)}$ $Y=[1,2,\ldots,Q+1,\ldots,2,1]_{(2Q+1)\times1}$ and the three-dimensional diagram of its weight matrix is indicated in Figure 5(a). It can be seen here that this weight calculation method is not isotropic. Gaussian function satisfies the requirements that the central pixel is emphasized and that the pixel which is closer to the central pixel has bigger weight. The sum of the normalized weights is 1 and it is isotropic. Its weight calculation formula is as follows:

$$[\mu(a,b)]_{(2P+1)\times(2Q+1)}=e^{\left(-\frac{X^2+Y^2}{2\pm^2}\right)} \tag{16}$$

Here, $\pm$ is the variance and its three-dimensional diagram is shown as Figure 5(b).

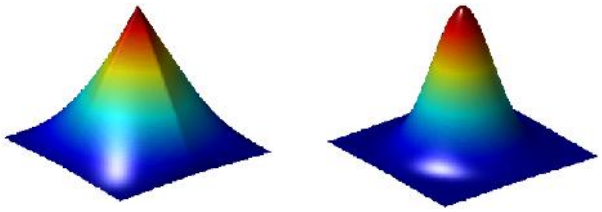

(a) Weight of literature [13] (b) Gauss weight

Figure 5. Weight function

Gauss weight SML is demonstrated as Formula (17):

$$WSML^{l,k}(i,j)=\sum_{a=-P}^{P}\sum_{b=-Q}^{Q}\mu(a,b)\left[ML^{l,k}(i+a,j+b)\right]^2 \tag{17}$$

Here, weight function $\mu(a,b)$ takes value according to Formula (16). Assuming that the high-frequency coefficients of the source image are $H_A^{l,k}$ and $H_B^{l,k}$, the fused coefficient is $H_F^{l,k}$ and the fused coefficient and weight are indicated as Formula (18) and (19):

$$H_F^{l,k}=W_{WSML}^{A}H_A^{l,k}+W_{WSML}^{B}H_B^{l,k} \tag{18}$$

$$W_{WSML}^{A}=\frac{WSML_A^{l,k}}{WSML_A^{l,k}+WSML_B^{l,k}} \quad W_{WSML}^{A}=1-W_{WSML}^{A} \tag{19}$$

4. Experiment Result and Analysis

4.1. Objective Evaluation Criteria of Image Fusion

The evaluation indexes of image fusion include entropy, standard deviation, average gradient and spatial frequency. Their specific definitions are clarified as follows:

Entropy: it measures the amount of information in the image.

$$E=-\sum_{i=0}^{L-1}p_i\log p_i \tag{20}$$

Here, p_i is the possibility that the pixel value i appears in the image.

Standard deviation: it measures the brightness fluctuation of the image and it shows the visual contrast. «$_{I_F}$ is the average brightness of the image.

$$\pm=\sqrt{\frac{1}{M\times N}\sum_{i=1}^{M}\sum_{j=1}^{N}\left(I_F(i,j)-«_{I_F}\right)^2} \tag{21}$$

Average gradient: it measures the image definition.

$$\nabla \overline{g} = \frac{\sum_{i=1}^{M}\sum_{j=1}^{N}\sqrt{\frac{\nabla_i^2 I_F(x,y) + \nabla_j^2 I_F(x,y)}{2}}}{(M-1)(N-1)} \tag{22}$$

Spatial frequency: it measures the image detail information.

$$SF = \sqrt{F_{RF}^2 + F_{CF}^2} \tag{23}$$

Here, F_{RF} and F_{CF} represent the horizontal and vertical frequencies.

$$F_{RF} = \sqrt{\frac{1}{MN}\sum_{i=0}^{M-1}\sum_{j=1}^{N-1}\left[f(i,j) - f(i,j-1)\right]^2} \tag{24}$$

$$F_{CF} = \sqrt{\frac{1}{MN}\sum_{j=0}^{N-1}\sum_{i=1}^{M-1}\left[f(i,j) - f(i-1,j)\right]^2} \tag{25}$$

4.2. Experiment Result and Analysis

This section compares the fusion effects different fusion algorithms play on the infrared and visible images. The fusion methods used are shown in Table 1 and the high-frequency coefficients all use congruency test [14]. The fusion results are indicated in Figure 6, 7 and 8. This paper evaluates the entropy, standard deviation, average gradient and spatial frequency of the fusion results and the evaluation result is indicated in Table 2.

Table 1. Fusion Methods

Fusion Method	Low-frequency Coefficients	High-frequency Coefficients
1	Take the average value	Take the maximum absolute value
2	Literature [7]	Maximum region energy
3	Weight GPC	Maximum region energy
Method of This Paper	Weight GPC	Weight SML

Visible image

Infrared image

Fusion method 1

Fusion method 2

Fusion method 3

The method of this paper

Figure 6. Fusion result (1)

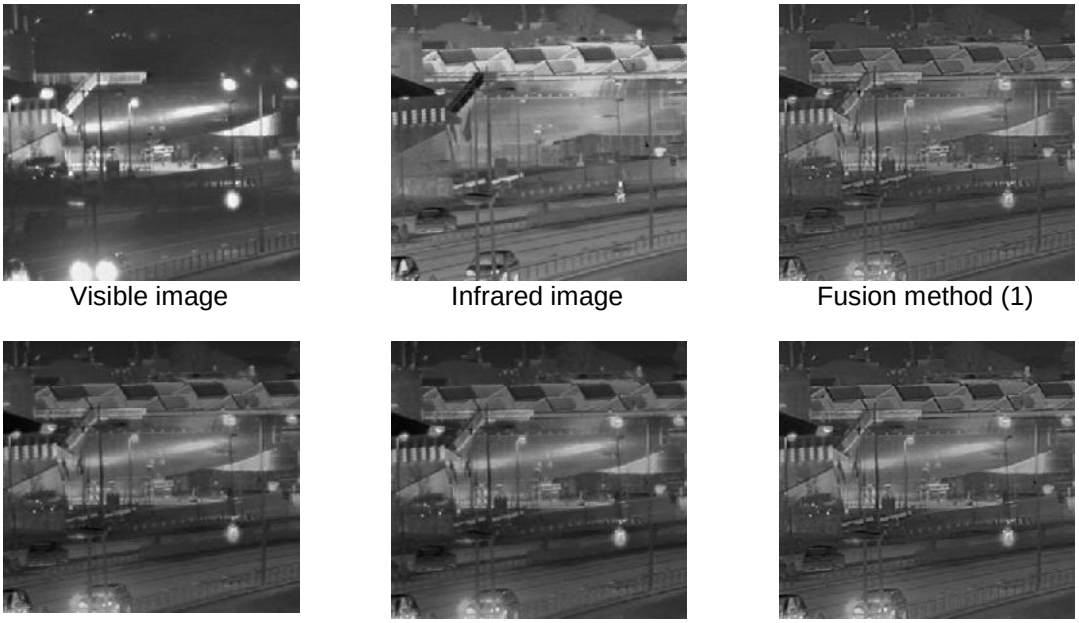

Visible image | Infrared image | Fusion method (1)
Fusion method (2) | Fusion method (3) | The method of this paper

Figure 7. Fusion result (2)

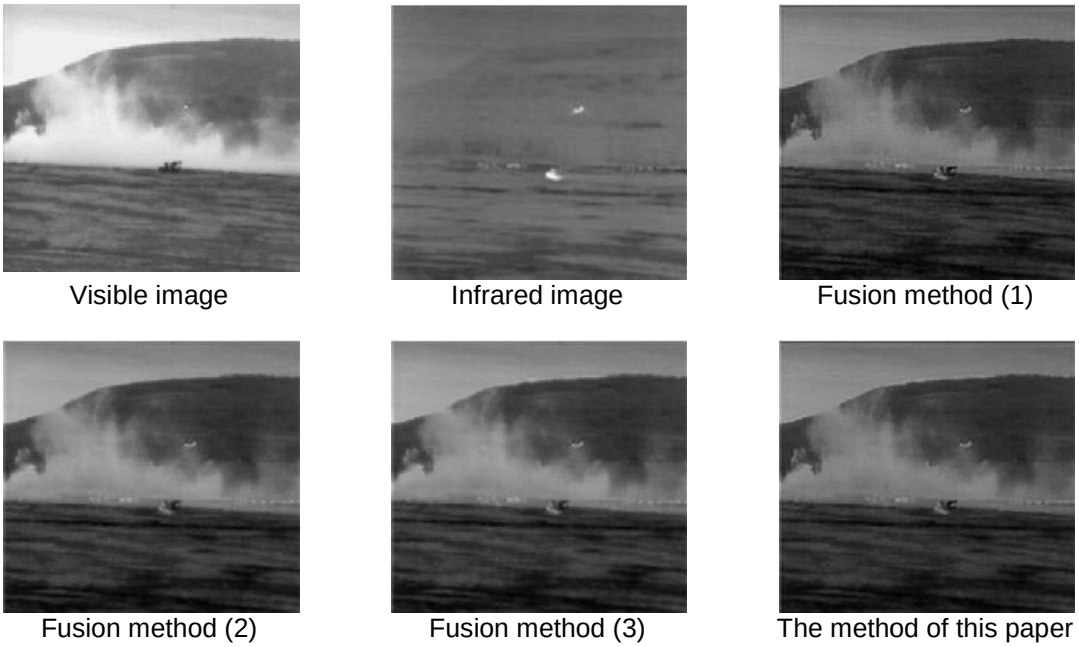

Visible image | Infrared image | Fusion method (1)
Fusion method (2) | Fusion method (3) | The method of this paper

Figure 8. Fusion result (3)

From the experiment result, it can be seen that the fusion effect by the method of this paper is better than the other three fusion methods. In the low-frequency coefficient fusion, the fused image by taking the average value is quite fuzzy. The method to use image quality evaluation in Literature [7] loses some image structure information while the low-frequency coefficient fusion method by using the correlation coefficients and GWPC in this paper effectively preserves the structure information of the infrared and visible images. As for the high-frequency coefficient fusion, the method to take the maximum absolute value based on point operation is bad in anti-noise performance. The method based on region operation has better

anti-noise performance while the processing method of this paper in the high frequency maintains more detail information compared to other methods.

5. Conclusion

This paper decomposes infrared and visible images by using NSCT to obtain image frequency domain representation in scales and it fuses the low- and high-frequency coefficients through the combination of correlation coefficient and weight GWPC and Gaussian weight SML respectively. Both the low- and high-frequency coefficient fusions have taken the influence the position information plays on the fusion result into consideration. The fusion experiment of the standard test image shows that the method of this paper better preserves the structural information of the original image and the high-frequency detail information, fuses the imaging features of the infrared and visible images, improves the visual effect and lays a solid foundation for the follow-up image analysis.

References

[1] Starck JL, Candès EJ, Donoho DL. The Curvelet Transform for Image Denoising. *IEEE Transactions on Image Processing.* 2002; 11(6): 670-684.
[2] Da Cunha AL, Zhou J, Do MN. The Nonsubsampled Contourlet Transform: Theory, Design, and Applications. *IEEE Transactions on Image Processing*. 2006; 15(10): 3089-3101.
[3] Zhao Chunhui, Ma Lijuan, Shao Guofeng. An Image Fusion Algorithm using WA-WBA and Improved INSCT. *Journal of Electronics and Information*. 2014; 36(2): 304-311.
[4] Adu J, Gan J, Wang Y, et al. Image Fusion Based on Nonsubsampled Contourlet Transform for Infrared and Visible Light Image. *Infrared Physics & Technology*. 2013; 61: 94-100.
[5] Yin M, Liu W, Zhao X, et al. A Novel Image Fusion Algorithm Based on Nonsubsampled Shearlet Transform. *Optik-International Journal for Light and Electron Optics*. 2014; 125(10): 2274-2282.
[6] Liu Yushu. Research on Image Denoising and Fusion Algorithm Based on Multi-scale Transform. Disertation. Jinan & Shandong University; 2013.
[7] Gao Yinhan, Chen Guangqiu, Liu Yanyan. Adaptive Image Fusion Based on Image Quality Assessment Parameter in NSST System. *Journal of Jilin University (Engineering Edition).* 2014; 6(1): 225-234.
[8] Wang Z, Bovik AC, Sheikh HR, et al. Image Quality Assessment: from Error Visibility to Structural Similarity. *IEEE Transactions on Image Processing*. 2004; 13(4): 600-612.
[9] Jingfeng MI, Qing Wu Li, Zhu Hao, et al. An Improved Image Quality Assessment Method Based on Structural Similarity. *Computer Technology and Development*. 2014; 24(3): 67-70.
[10] Jianhua Liu, Jianguo Yang, Beizhi Li. Multifocus Image Fusion by SML in the Shearlet Subbands. *TELKOMNIKA Indonesian Journal of Electrical Engineering*. 2014; 12(1): 618-626.
[11] Dexiang Hang. Fusion of Multiband SAR Images Based on Directionlet Transform. *TELKOMNIKA Indonesian Journal of Electrical Engineering*. 2014; 12(1): 506-513.
[12] Mahyari AG, Yazdi M. Panchromatic and Multispectral Image Fusion Based on Maximization of both Spectral and Spatial Similarities. *IEEE Transactions on Geoscience and Remote Sensing*. 2011; 49(6): 1976-1985.
[13] Yin M, Liu W, Zhao X, et al. A Novel Image Fusion Algorithm Based on Nonsubsampled Shearlet Transform. *Optik-International Journal for Light and Electron Optics*. 2014; 125(10): 2274-2282.
[14] Li H, Manjunath BS, Mitra SK. Multisensor Image Fusion using the Wavelet Transform. *Graphical Models and Image Processing*. 1995; 57(3): 235-245.